Structure Formation and Characterization of PVDF Hollow Fiber Membranes by Melt-Spinning and Stretching Method

Chun-Hui Du, You-Yi Xu, Bao-Ku Zhu

Department of Polymer Science and Engineering, Zhejiang University, Hangzhou 310027, China

Received 10 November 2006; accepted 27 May 2007
DOI 10.1002/app.26867
Published online 17 July 2007 in Wiley InterScience (www.interscience.wiley.com).

ABSTRACT: Melt-spinning and stretching (MS-S) method was proposed for preparing poly(vinylidene fluoride) (PVDF) hollow fiber membranes with excellent mechanical properties. The morphology and properties of PVDF fibers and membranes were investigated by small angle X-ray scattering (SAXS), differential scanning calorimeter (DSC), field emission scanning electron microscope, mercury porosimeter, and tensile experiment. SAXS results indicated that the stacked lamellar structure aligned normal to the fiber axis was separated and deformed when the fibers were strained, and the long period of the strained fibers increased accordingly. Factors affecting the membrane properties were mainly spin-draw ratio, annealing temperature, time, and stretching rate. Experimental results showed that the average pore size, porosity, and N_2 permeation of the membranes all increased with the increasing spin-draw ratios and annealing temperatures. Annealing the nascent PVDF hollow fibers at 145°C for 12 h was suitable for attaining membranes with good performance. In addition, the amount and size of the micropores of the membrane increased obviously with stretching rate. Tensile experiment indicated PVDF hollow fiber membranes made by MS-S process had excellent mechanical properties. © 2007 Wiley Periodicals, Inc. J Appl Polym Sci 106: 1793–1799, 2007

Key words: PVDF; fibers; membranes; morphology; melt spinning

INTRODUCTION

Poly(vinylidene fluoride) (PVDF) is one of the widely used fluoride-containing membrane materials, because of its very useful combination of processability, good mechanical strength, thermal and chemical stability, and radiation resistance. PVDF membranes as an important product have been widely used in industrial separation field,[1–4] and were usually prepared using thermally induced phase separation (TIPS)[5–7] and solution phase inversion methods.[8–10] However, the above two methods all can result in a waste solvent problem, and the mechanical properties of the membranes made by these methods were relatively poor (especially for the solution phase inversion method). Compared with TIPS and phase inversion processes, the melt-spinning and stretching (MS-S) process does not involve a large amount of organic solvent, and should be developed to prepare PVDF membranes.

Recently, PVDF fibers made by melt spinning process were extensively studied.[11–13] Samon et al.[11] studied the structure development of PVDF in the early stages of the melt spinning process and found that shish-kebob crystals aligned along the fiber and the defective shish-kebob structure eventually transforms into a well-defined lamellar structure. Wu et al.[12] studied the crystal development and mechanical behavior of PVDF fibers under deformation. They reported that crystallites linked by extended amorphous chains along the fiber axis coexisted with correlated microvoids. The tensile test indicated that necked and unnecked regions were developed alternately along the fiber after the yielding point at about 5–10% strain. Du et al.[13] studied the hard elasticity of PVDF fibers prepared by melt spinning and annealing process and found that the stacked crystalline lamellae aligned normal to fiber axis existed in the fibers, and the fibers also had a higher elastic recovery of 85% from 50% extension at the room temperature. However, PVDF hollow fiber membranes made by melt-spinning and stretching process have seldom been reported.

In fact, MS-S method has been a standard process for preparing the crystalline polymer membranes, such as polypropylene (PP) and polyethylene (PE)

Correspondence to: B.K. Zhu (zhubk@zju.edu.cn).
Contract grant sponsor: National 973 Foundation of China; contract grant number: 2003CB615705.
Contract grant sponsor: NSFC; contract grant number: 50433010.
Contract grant sponsor: China Postdoctoral Science Foundation; contract grant number: 2005038629.

membranes.[14–16] For MS-S method, a pure polymer melt is spun, and the micropores of the membranes by MS-S process are formed by the mechanical force acting on the membranes in the subsequent stretching step. This means that the MS-S process does not involve any phase separation and its handling is relatively easy. The mechanism of forming microvoids is due to the stacked crystalline lamellae aligned normal to the fiber axis. When the fiber is stretched, the crystal lamellae are separated with the formation of a large amount of interconnected voids. Thus, the micropore structure is formed by the stress and then it is completed during annealing.[9] So the crystal structure was the most important factor to be considered before preparing PVDF membranes by the MS-S process. In the former studies,[13,17] we found that PVDF fibers made by melt-spinning and annealing process had stacked crystalline lamellae and higher elastic recovery, which meant that PVDF may be prepared into membranes through MS-S method just as PP and PE.

In this paper, PVDF hollow fiber membranes were prepared by MS-S process. The effects of melt-spinning and stretching conditions such as spin-draw ratio, annealing, and stretching rate on the morphology and properties of PVDF hollow fibers and membranes are the objectives of this study and are discussed in detail later.

EXPERIMENTAL

Materials

Extrusion grade PVDF (melting point 173°C), supplied by Zhejiang Lantian Co (Hangzhou, China), contains no nucleating agents. The melt flow index is 1.9 g/10 min (230°C, 5 kg load). Its weight-average molecular weight and polydispersity index M_w/M_n are 3.3×10^5 and 1.99, respectively.

Preparation of PVDF hollow fiber membranes

A single screw extruder were used for melt spinning; it has four zones with a temperature of zone 1 at 160–190°C, zone 2 at 200–230°C, zone 3 at 230–250°C, and zone 4 at 220–240°C. A tube-in orifice spinneret with inner and outer diameters of 15 and 22 mm was used. First, PVDF melts were extruded out of the spinneret at 210–240°C by using nitrogen as bore gas. Then, the hollow fibers were taken up at a spin-draw ratio of 900–1600 and then annealed. If no special explanation, the annealing temperature and time were chosen as 145°C and 12 h. Subsequently, the hollow fibers were strained to 10–30% extension at temperatures lower than 40°C and then to 120% extension at temperatures higher than 80°C. At last, the hollow fibers were heat-set at 150°C for 30 min. The preparation can be described as shown in Scheme 1.

Degree of Crystallinity from DSC

A Perkin-Elmer Pyris-1 DSC was used to measure the crystallinity (X_c) of the sample at a heating rate of 10°C/min. The crystallinity was defined as:

$$X_c(\%) = \frac{\Delta H}{\Delta H^0} \times 100 \quad (1)$$

where ΔH is the measured heat of fusion for the sample, and ΔH^0 is the theoretical heat of fusion for the pure PVDF crystal (taken as 104.7 J/g).[18,19]

Morphologies and crystal structure of the samples

The morphology of the samples was examined by using a FEI SIRION field emission scanning electron microscope. The surfaces of the samples were coated with gold prior to examination. The crystal structure of the samples was investigated by a small-angel X-ray scattering (SAXS) (Bucker D8 Discover GADDS) with Cr radiation (λ = 0.229 nm). The SAXS measurement was performed on a small bundle of PVDF hollow fibers and the direction of X-ray was perpendicular to the fiber axis.

N_2 Permeation

The N_2 permeation was measured by a laboratory made gas permeation device, the nitrogen pressure was controlled as 0.6 MPa. The N_2 permeation (J_{N2}) was calculated according to the following equation[20]:

$$J_{N_2} = \frac{V_{N_2}}{A \times P \times t} \quad (2)$$

where V_{N_2} is the nitrogen volume that permeates through the membrane, A is the membrane area that is calculated on the basis of the inner diameter of the hollow fiber membrane, P is the nitrogen pressure between the upside and downside of the membrane, and t is the time when nitrogen permeates through the membrane.

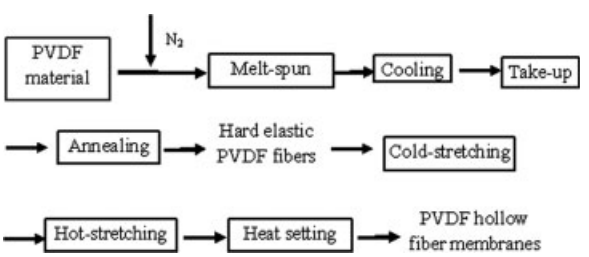

Scheme 1 Preparation process of PVDF hollow fiber membranes.

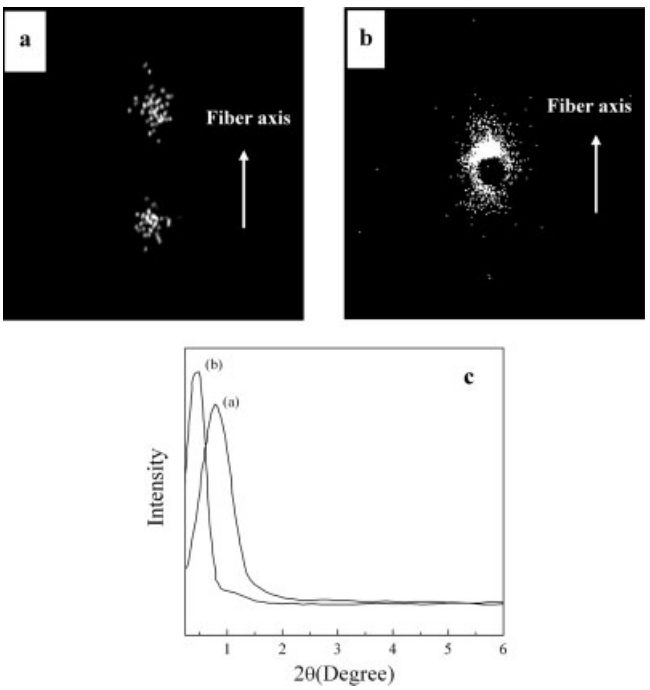

Figure 1 SAXS patterns and curves for PVDF fibers. (a) unstrained fibers; (b) strained fibers.

Porosity

The porosity and average pore size of the membranes were measured using a mercury porosimeter (Micrometrics Autopore IV 9510).

Mechanical testing

Mechanical properties of PVDF hollow fibers were measured by an electronic tensile tester (AG-1, Japan). All the tests were conducted at 20°C and 60% relative humidity. Elastic recovery was determined along stretched direction of the fiber under the first cycle of loading and unloading at a deformation rate of 120% min^{-1}.The percent elastic recovery of the fiber can be calculated according to our former report.[13]

RESULTS AND DISCUSSION

Crystal structure

The crystal structure of strained PVDF samples was examined by SAXS measurement as shown in Figure 1. The pattern of unstrained PVDF hollow fibers [Fig. 1(a)] showed a two-point pattern, which indicated that the crystals existed in the form of crystalline lamellae and the lamellar planes were perpendicular to the fiber axis.[13,17] The corresponding diffraction intensity curve of the unstrained fibers indicates a primary scattering peak at $2\theta = 0.78^\circ$ as shown in Figure 1(c), curve a, which corresponded to a *d*-spacing of 16.8 nm. Compared to unstrained PVDF hollow fibers, the two-point pattern cannot be distinguished clearly, as shown in the SAXS pattern of strained PVDF samples [Fig. 1(b)]. The scattering curve for strained PVDF fibers showed a primary scattering peak at $2\theta = 0.46^\circ$, which corresponded to a long period of 28.5 nm [curve b in Fig. 1(c)]. It was indicated that the long period of the fibers increased distinctly when compared to the unstrained fibers. The morphological properties of the strained PVDF samples suggested that the crystalline lamellae were separated and deformed in the direction of stretching under the stress, thus the pore structures in the fiber wall were formed.[21] The pore structures of the samples were affected by many factors such as spin-draw ratio, annealing process, and stretching rate, which will be examined in the following studies.

Effect of spin-draw ratio

The effect of spin-draw ratio on the resulting hollow fiber properties was investigated and the results are exhibited in Figure 2 and Table I. Figure 2 shows that the crystallinity of PVDF hollow fibers increases greatly with increasing spin-draw ratios. The spin-draw ratio also had great influences on the elastic recovery of the fibers. When the spin-draw ratio was below 1400, the elastic recovery increased with the spin-draw ratios, and then it decreased with the increasing spin-draw ratio, as shown in Figure 2. In addition, the average pore sizes, porosity, and N_2 permeations of the PVDF hollow fiber membranes all increased with increasing spin-draw ratios, as exhibited in Table I.

The explanation for the phenomena might be that higher spin-draw ratio can increase the orientation of the fibers and stimulate the formation of more perfect row-nucleated crystals, which increased the

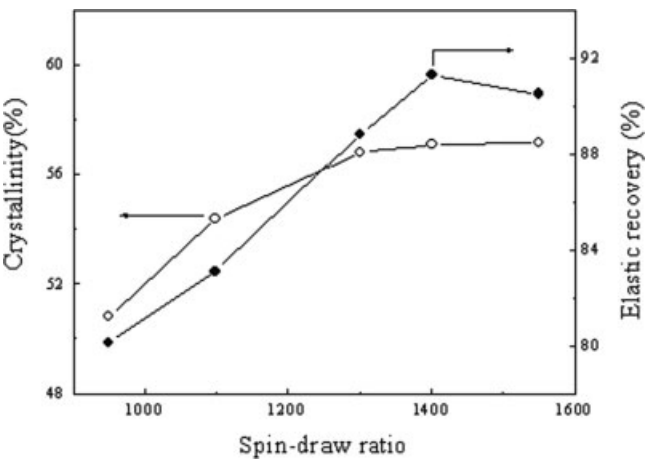

Figure 2 Effects of spin-draw ratios on crystallinity and elastic recovery of PVDF hollow fibers.

TABLE I
Properties of PVDF Hollow Fiber Membranes with Different Spin-Draw Ratio

Spin-draw ratio	Inner diameter (μm)	Thickness of the membrane (μm)	Average Pore diameter (nm)	Porosity (%)	J_{N2} (cm^3/cm^2 s cmHg)
1099	260	78	17.2	17.5	1.16×10^{-6}
1400	245	65	21.4	22.6	1.12×10^{-5}
1550	240	60	23.6	25.3	1.53×10^{-5}

crystallinity of PVDF hollow fibers. The elastic recovery was related with the crystallinity and the mobility of noncrystalline regions of the fibers.[13] When the spin-draw ratio was below 1400, the orientation of the crystalline and noncrystalline region all increased with the spin-draw ratio, which would result in the increases of the crystallinity and the mobility of the noncrystalline region of the fibers. Thus, the elastic recovery of the fibers increased with the spin-draw ratio. When the spin-draw ratio was above 1400, further increase of the crystallinity can decrease the mobility of noncrystalline region of the fibers, which would result in a little decrease of the elastic recovery. So, the choice of proper spin-draw ratio was important for the elastic recovery. Besides, with the increasing crstallinity, more perfect crystalline lamellae were in favor of the formation of more and large pores in the fiber wall, which increased the porosity and gas permeation of the membranes. The SEM micrographs of the resulting hollow fiber membranes spun with spin-draw ratios of 1099, 1400, and 1550 are exhibited in Figure 3. It was indicated that the micropores of the hollow fiber spun with spin-draw ratio of 1550 were more and larger than those of the hollow fiber spun with spin-draw ratio of 1099. These results further indicated that the spin-draw ratios have great effects on the membrane structure and performances.

Effect of annealing

The annealing temperature and time all have great influences on the structure and performance of the resulting hollow fibers, as shown in Table II. It was

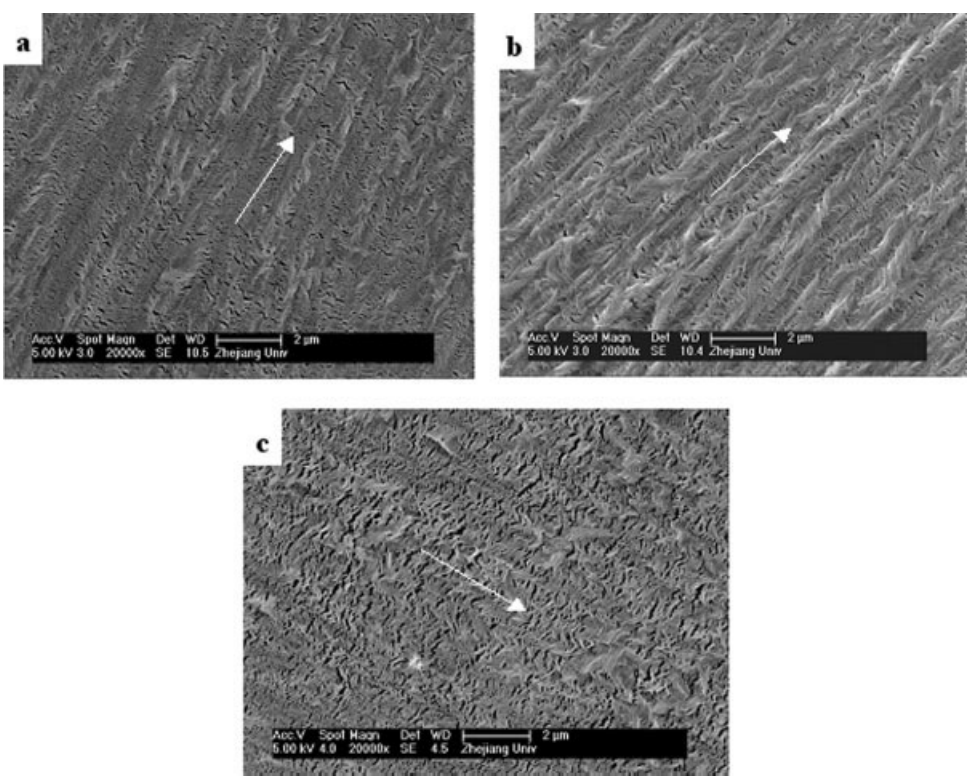

Figure 3 SEM photographs of inner surface of PVDF hollow fiber membranes with different spin-draw ratios. (a) 1099; (b) 1400; (c) 1550, the stretching rate is 120 mm/min (the arrow indicates the extrusion direction).

TABLE II
Properties of PVDF Hollow Fibers Annealed at Different Temperature for 12 h, the Spin-Draw Ratio of the Fiber is 1400

	Hollow fibers before straining		Hollow fibers after straining	
Annealing temperature (°C)	Er (%)	Crystallinity (%)	N_2 permeation[a]	Porosity (%)
No annealing	61	49.6	–	–
110	75	50.8	–	12.5
120	80	52.3	0.15×10^{-5}	16.1
130	86	53.7	0.96×10^{-5}	20.3
150	92	56.5	1.18×10^{-5}	22.7

[a] Unit of N_2 permeation is cm^3/cm^2 s cmHg.

indicated that the elastic recoveries of the annealed PVDF hollow fibers enhanced to a great extent in contrast to the unannealed fibers. Besides, the crystallinity of the unstrained hollow fibers increased with increasing annealing temperatures. This might be that higher annealing temperature was in favor of the rearranging of imperfect crystals, which were formed by the stress-induced crystallization in the melt spinning process. As a result of improved elasticity, the micropores in the fiber wall formed more easily when the hollow fiber was strained, the porosity and N_2 permeation of the hollow fiber membrane both increased with increasing annealing temperature. In addition, the effect of annealing time on the unstrained hollow fibers was examined in this study. Figure 4 showed that the crystallinity and elastic recovery of the hollow fibers increased with increasing annealing time in about 12 h. However, more annealing time had almost no influence on the elastic recovery and crystallinity of the hollow fiber. The explanation might be that the reordering of the molecular chains in the fiber wall was a dynamic process, which needed some time to fulfill. Once the process was mostly completed, increasing the annealing time further had no effect.[20] On the basis of the results, it was indicated that about 12 h of annealing was proper for obtaining PVDF hollow fibers with good performances.

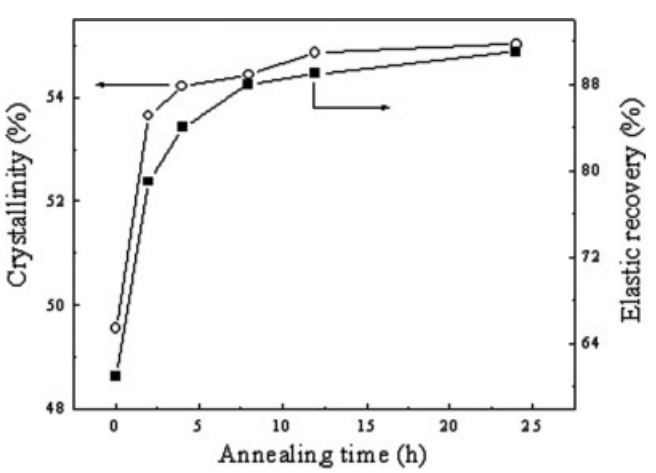

Figure 4 Effects of annealing time on crystallinity and elastic recovery of PVDF hollow fibers, the annealing temperature is 145°C.

Effect of stretching rate

The effects of stretching rate on the morphology of PVDF hollow fiber membranes were examined in this study. Figures 5 and 3(b) showed the SEM photographs of inner surface of PVDF hollow fiber membranes at different strain rate. It was indicated that no pore structure was found in the unstretched fiber wall [Fig. 5(a)]. As for the stretched samples, the amount of the pores in the fiber wall was relatively small at lower strain rate, and then it increased obviously with increasing strain rate. Besides, the pore size increased with increasing strain rate and the distribution of the pore become more uniform. These results might be explained by the fact that at a faster strain rate, the relaxation of molecular chains was inhibited, thus more defects were formed, which resulted in more micropores formation in the fiber wall. Moreover, the faster strain rate can destroy the skin structure, stimulating the formation of cracked pore structure in the fiber wall. Thus, the amount and size of the micropores increased with the increasing strain rate.

In the study, the pore size and N_2 permeation of the membranes was relatively small, but it indicated the possibility of using MS-S method to prepare PVDF hollow fiber membranes.

Mechanical properties

The stress–strain curves of PVDF hollow fibers and membranes are shown in Figure 6, the spin-draw ratio of the samples is 1400, and the membrane sample was the same as that in Figure 3(b). It was indicated that PVDF membranes [Fig. 6(b)] had excellent mechanical properties, its breaking strength reached 213 MPa, and its breaking strain was about 20% at the room-temperature stretching conditions. Compared to PVDF membranes, the breaking strength and

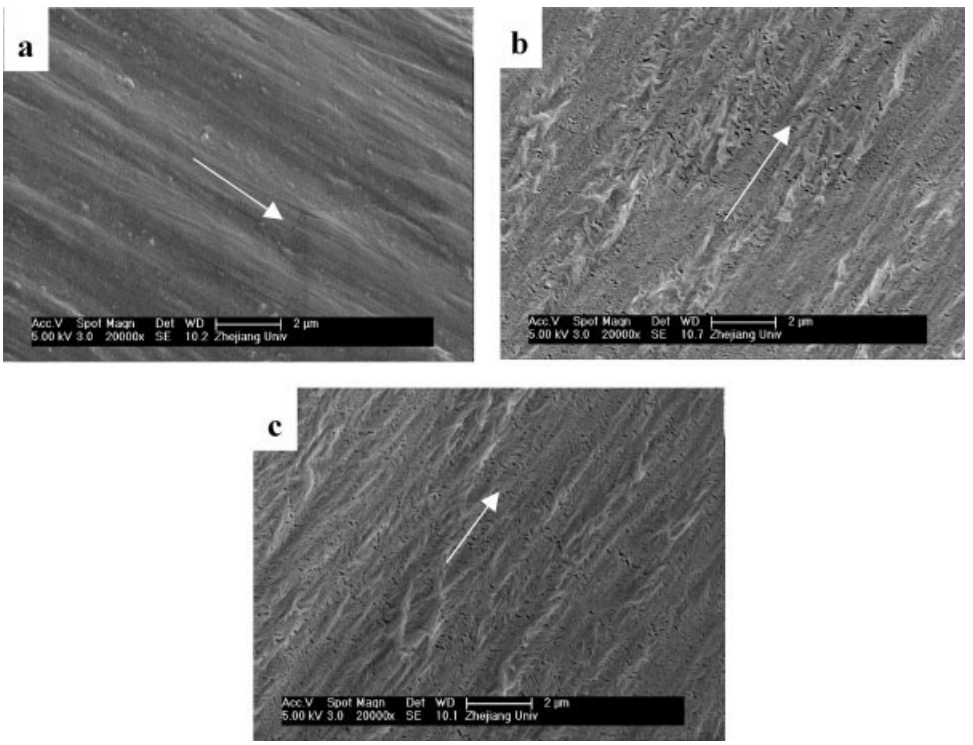

Figure 5 SEM photographs of inner surface of PVDF hollow fiber membranes at different stretching rates (mm/min): (a) 0; (b) 30; and (c) 90. The arrow indicates the extrusion direction, the spin-draw ratio is 1400.

strain of PVDF fibers [Fig. 6(a)] were 123 MPa and 80%, respectively. The mechanical properties indicated that PVDF hollow fiber membranes prepared by MS-S method had excellent breaking strength, which was much higher than that of the membranes made by solution phase inversion and TIPS method, their breaking strength were in the range of 0–10 MPa and 7–20 MPa, respectively.[6]

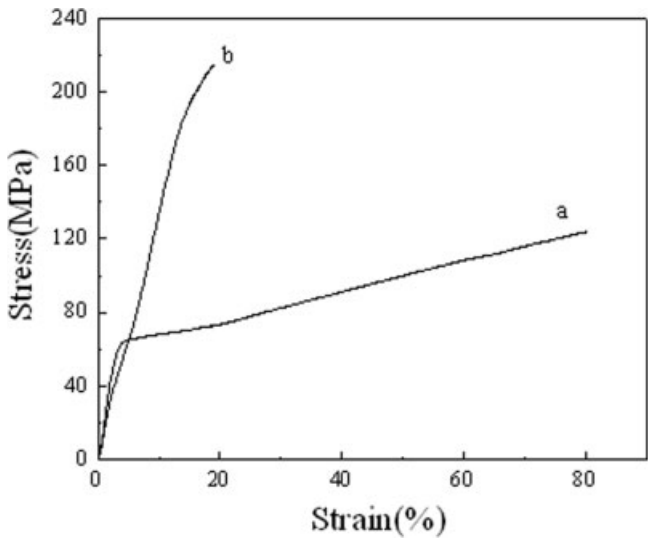

Figure 6 Stress–strain curves of PVDF hollow fiber (a) and membrane (b), the extension rate is 120% min^{-1}.

CONCLUSIONS

PVDF hollow fiber membranes were prepared by melt-spinning and stretching process. The results indicated that the stacked lamellar structure aligned in the direction normal to the fiber axis was separated and deformed when the fibers were strained, and the long period of the strained fibers increased accordingly. With the spin-draw ratio increasing, the average pore sizes and N_2 permeations of the membranes increased, and they reached 23.6 nm and 1.53×10^{-5} cm^3/cm^2 s cmHg, respectively. Annealing the nascent PVDF hollow fibers at 145°C for 12 h was suitable for attaining membranes with good performance, and higher annealing temperature also increased the porosity and N_2 permeations of the membranes. Moreover, the amount and size of the micropores in the fiber wall increased with stretching rate. PVDF hollow fiber membranes exhibited excellent mechanical properties, its breaking strength reached 213 MPa, which was much higher than that of the membranes made by solution phase inversion and TIPS method.

References

1. Kong, J. F.; Li, K. J Membr Sci 1999, 16, 83.
2. Jian, K.; Pintauro, P. N. J Membr Sci 1997, 135, 41.
3. Chabot, S.; Roy, C.; Chowdhury, G.; Matsuura, T. J Appl Polym Sci 1997, 65, 1263.

4. Ademovic, Z.; Klee, D.; Kingshott, P. J Biomol Eng 2002, 19, 177.
5. Takamura, M.; Yoshida, H. US Pat. 6,299,773 (2001).
6. Doi, Y.; Matsumura, H. US Pat. 5,022,990 (1991).
7. Smith Samantha, D.; Shipman Gene, H.; Floyd, R. M.; Freemyer, H. T.; Hamrock, S. J.; Yandrasits, M. A.; Walton, G. S. WO Pat. 035,641 (2005).
8. Wang, D. L.; Li, K.; Teo, W. K. J Membr Sci 2000, 178, 13.
9. Wang, D. L.; Li, K.; Teo, W. K. J Membr Sci 2000, 163, 211.
10. Khayet, M.; Feng, C. Y.; Khulbe, K. C.; Matsuuia, T. Polymer 2002, 43, 3879.
11. Samon, J. M.; Schultz, J. M.; Hsiao, B. S.; Seifert, S.; Stribeck, N.; Gurke, I.; Saw, C.; Collins, G. Macromolecules 1999, 32, 8121.
12. Wu, J.; Schultz, J. M.; Yeh, F.; Hsiao, B. S.; Chu, B. Macromolecules 2000, 33, 1765.
13. Du, C. H.; Zhu, B. K.; Xu, Y. Y. Macromol Mater Eng 2005, 290, 786.
14. Kamada, K.; Minami, S.; Toshida. K. US Pat. 4,055,696 (1977).
15. Kim, J. J.; Jang, T. S.; Kwon, Y. D.; Kim, U. Y.; Kim, S. S. J Membr Sci 1994, 93, 209.
16. Shino, M.; Yamamoto, T.; Fukunage, O.; Yamamori, H. US Pat. 4,530,809 (1985).
17. Du, C. H.; Zhu, B. K.; Xu, Y. Y. J Mater Sci 2005, 4, 1035.
18. Wang, Y. D.; Cakmak, M. J Appl Polym Sci 1998, 68, 909.
19. Nakagawa, K.; Ishida, Y. J Polym Sci Polym Phys Ed 1973, 11, 2153.
20. Shen, L. Q.; Xu, Z. K.; Xu, Y. Y. J Appl Polym Sci 2003, 84, 203.
21. Cannon, S. L.; Mckenna, G. B.; Statton, W. O. J Polym Sci Part D: Macromol Rev 1976, 11, 209.